Grain-size analysis of mudrocks: A new semi-automated method from SEM images

Accepted Manuscript

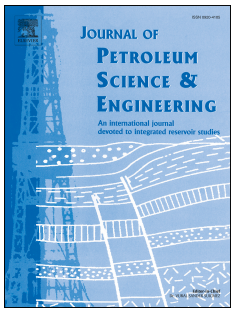

Grain-size analysis of mudrocks: A new semi-automated method from SEM images

Shereef A. Bankole, Jim Buckman, Dorrik Stow, Helen Lever

PII: S0920-4105(18)31018-0

DOI: https://doi.org/10.1016/j.petrol.2018.11.027

Reference: PETROL 5499

To appear in: *Journal of Petroleum Science and Engineering*

Received Date: 31 October 2017

Revised Date: 2 November 2018

Accepted Date: 12 November 2018

Please cite this article as: Bankole, S.A., Buckman, J., Stow, D., Lever, H., Grain-size analysis of mudrocks: A new semi-automated method from SEM images, *Journal of Petroleum Science and Engineering* (2018), doi: https://doi.org/10.1016/j.petrol.2018.11.027.

Grain-size analysis of mudrocks:

A new semi-automated method from SEM images

Shereef A. Bankole[a,b*], Jim Buckman[a], Dorrik Stow[a] and Helen Lever

[a]Institute of Petroleum Engineering, Heriot-Watt University, Edinburgh, EH14 4AS United Kingdom.

[b]Department of Chemical and Geological Sciences Al-Hikmah University, P.M.B 1601, Nigeria.

Keywords: Grain size; SEM; mudrocks; microstructure, image analysis

Abstract

There is a growing interest in mudrocks as a result of their potential as hydrocarbon reservoirs, in the storage of carbon dioxide, and as repositories for nuclear waste. Methods for characterising mudrocks are fast evolving in order to better characterise their very small grain sizes. Grain-size analysis of mudrock is challenging and time-consuming and there is need to develop a fast, effective and objective method for accurately determining the grain size of this group of rocks. We suggest that this is best achieved by using high-resolution electron microscopy to study both the microstructure and grain size of mudrocks at the same time.

The contribution presents grain-size analysis from scanning electron microscopy (SEM) through image analysis of the Feret (or calliper) diameter of grains. The method has been tested on 7 mudrock samples from two IODP Expeditions and compared with results from standard laser diffraction granulometry. Image analysis shows that all the samples fall within the clayey silt to silty clay range with average grain size from fine silt to medium silt. Closely comparable results and statistical parameters were obtained by laser diffractometry. Linear plots of grain percentage at corresponding phi values show strong positive correlation between the two techniques with R-square values typically ranging between 0.76 and 0.96. Image analysis of grain size as described herein gives comparable and generally smoother normal distribution curves than the laser diffraction technique for all the seven samples.

The procedures involved in the proposed method for analysing grain size of fine-grained sediments are rapid, automated, devoid of human subjectivity and precise.

1. Introduction

Grain size is a fundamental property of rock which has a constitutive effect on the petrophysical properties such as surface area, pore size distribution, porosity and permeability. There is a positive correlation between grain size and pore size distribution with a subsequent effect on fluid movement within the rock (Aplin et al., 1999; Yang and Aplin, 2007). Grain size distribution reflects the hydrodynamic condition of the depositional environment (Saner et al., 1996) hence it is a useful forensic technique to reconstruct the depositional processes and mode of transport of sediments (Blott et al., 2004).

Numerous techniques have been developed for analysing the grain size of sediments, including sieving, laser diffraction, dynamic light scattering, image analysis, sedimentation, and electro zone sensing among others. The choice of technique depends in part on the grain

size of the material, but in most cases the technique should be accurate, inexpensive, fast and cover a wide range of grain sizes (Jiang and Liu, 2011).

However, grain-size analysis of fine-grained sediment is especially difficult and time consuming. There is a strong possibility of underestimating the proportion of clay-size particles (< 4 um) due to the fact that clay particles are within the resolution limit of most equipment (Røgen et al., 2001). Recognition of mudrocks as important hydrocarbon reservoirs (shale gas and shale oil), as potential storage containers for carbon dioxide in the subsurface and as repositories for nuclear waste has put into sharp focus a growing interest in studying mudrocks. This has prompted an on-going development of methods that are suitable for analysing this suite of rocks.

Electron microscopy has been employed in resolving features down to the nanometre scale and it is a common method utilised in studying both the nanostructure and microstructure of fine-grained sediments (Camp and Wawak, 2013; Curtis et al., 2010; Ji et al., 2017). These techniques can also be used in quantifying mudrock grain size, although such application is relatively rare. The scarcity of utilising electron microscopy imaging in estimating the grain size might be due, in part, to the limited area of coverage normally obtained by the scanning electron microscopy (SEM) method and hence how representative the measurement is of the whole sample (Sanei et al., 2016; Saraji and Piri, 2015).

In this study, in order to mitigate against the issue of a very small measurement area, grain size analysis was carried out with large-scale images (ca. 0.65 mm X 0.42 mm) acquired from polished thin sections through backscattered electron (BSE) imaging of the scanning electron microscope. The grain size analysis results from image analysis described herein were compared with grain size analysis results using laser diffraction granulometry on the same samples.

2. Principal Methods of Grain-Size Analysis

There are several principal techniques for measuring the grain size of sediments (including soils) and sedimentary rocks. Each technique measures a different property of the sediment and then relates this property to the grain diameter (or grain volume) of constituent particles. The amount of sediment in each of the different size classes (as originally proposed by Wentworth, 1922) is reported as a fraction of the total amount of sediment analysed in one of three ways: (a) as a volume percentage of the total volume; (b) as a weight percentage of the total dry weight; or (c) as the absolute number of particles counted.

The principal techniques can be summarised as follows (Figure 1).

1. *Laser diffraction*. Particle size analysis by laser diffraction is currently one of the most common methods employed in sedimentology. It is based on the premise that particle size determines the angle of light diffraction. There is a negative correlation between the diffracted angle and particle size, such that a small size particle produces a higher diffraction angle compared with a larger particle size (Figure 2).

A laser light source is generally directed through a small, dilute, liquid suspension of the sediment dispersed in distilled water and the diffraction angle of different grains is measured. Samples of about 100 - 500 mg are introduced into the water module of the laser equipment. The technique is most appropriate for unconsolidated sediments and readily measures grain

sizes between 100 nm and 5 mm. The laser diffraction technique can also be used to analyse samples in a dry state.

2. *Image analysis*. This is the only method that makes direct measurement of grain diameter (known as the Feret or Calliper diameter). It is commonly performed in conjunction with analysis of microfabric and grain orientation. Grain size through image analysis requires image acquisition, processing, measurement and then interpretation (Francus, 1998). The method can be performed on both sedimentary rocks (polished thin-section) and unconsolidated sediment. Images are acquired using a high-resolution camera in the field or lab for gravel size particles or with a camera attached to an optical microscope (for sandy sediments) and a scanning electron microscope (for sand to clay size particles). Sample sizes required for analysis can be as small as 2 to 5 g for polished thin-sections and < 100 mg for unconsolidated sediment.

Image analysis generally refers to a computer-automated technique, and is therefore considered to be objective, precise and reproducible. It can measure accurately between 10 nm and 5 mm, but this is dependent on the equipment used (Bons and Jessell, 1996). Manual image analysis by direct observer measurement and point-counting of grains in thin sections or smear slides is typically used for grain sizes between 0.03 mm and 1 mm.

3. *Sedimentation*. There are a number of techniques that apply sedimentation through a water column in analysing the grain sizes present in sediments and soils. These methods are all based on the principle of relating the settling velocity of grains in distilled water to the diameter of the grains. Sediments are introduced to the top of a tube containing water and the settling rate of the grains is monitored at the base. The coarsest grains settle most rapidly, whereas the finest grains settle more slowly. The shape of the grains is assumed to be spherical and the sphere diameter is calculated using Stoke's law. The settling velocity is dependent on the shape and density of the grains (Lewis and McConchie, 1994). The technique requires a sample size of about 1 - 10 g for sandy sediments and < 1 g for silt to clay-rich sediment, and can accurately measure grain sizes between 100 nm and 100 um, depending on the particular techniques employed. The sediment must be unconsolidated or disaggregated.

4. *Sieving*. This is a common method used in analysing unconsolidated, coarse-grained sediments (0.05 mm to >50 mm). A sample size of between 30 - 70 g is introduced into a set of sieves which are arranged in descending order of mesh size. The set of sieves containing the sample is mechanically shaken for 10 to 15 minutes, and the weight of the fraction retained by each sieve size is then measured. Ultrasonic micro-sieving can be used with a particle analyser for the silt-size range (0.005 – 50 mm). Sieve analysis is only possible for unconsolidated sediments, or those that can be readily disaggregated prior to sieving.

Each method has clear advantages and disadvantages. Important considerations when selecting the appropriate technique include: sample size and how representative the sample is of a heterogeneous sediment.

Particle size range										
Technique	Principle	0.1nm	1nm	10nm	100nm	1µm	10µm	100µm	1mm	10mm
Laser diffraction	Scattered light									
Dynamic light scattering	Light Intensity									
Electrophoretic light scattering	Electrophoretic mobility									
Automated imaging	Grain diameter									
Sedimentation	Settling velocity									
Electrozone sensing	Resistivity									
Sieving	Grain diameter									

Figure 1. Different grain size techniques, their principles and resolution (From, Malverns Instruments Limited, 2012).

131

132

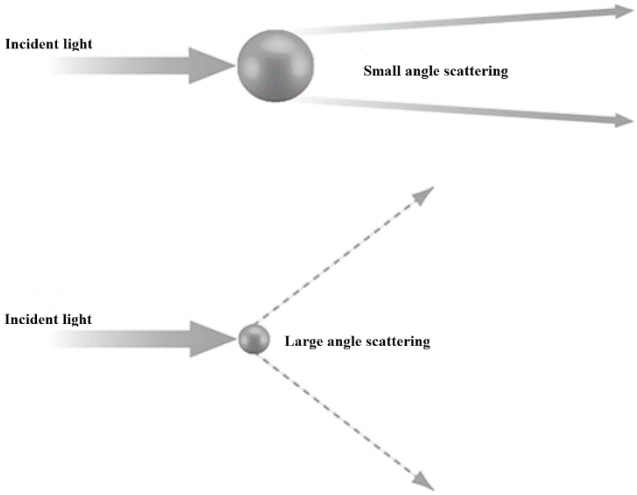

133 Figure 2. Diagram showing relationship between particle size and diffraction angle (Malverns
134 Instruments Limited, 2012).

3. Materials and methods

3.1. Samples

This study is part of a broader research programme investigating the microfabric of fine-grained sediments (mudrocks). It seeks to examine the relationship between microfabrics and depositional processes in deep-water. The samples used for this study are from core samples retrieved during Expeditions 317 and 339 of the International Ocean Discovery Program (IODP), from the Canterbury continental margin off New Zealand and the Iberian continental margin off SW Portugal and Spain, respectively. The samples were selected from the mud-rich hemipelagic intervals as follows:

- IODP 317, Site 1352, one sample from the continental slope, core depth 700m sub-sea floor.
- IODP 317, Site 1354, one sample from the continental shelf, core depth 130m sub-sea floor.
- IODP 339, Site 1385, five samples from the continental slope, core depth 100m sub-sea floor.

Two set of sub-samples were taken from each of these 7 samples to allow replicate measurements, through image analysis and laser diffraction. The samples are all from bioturbated, calcareous muds that are interpreted as the result of hemipelagic sedimentation. The Canterbury margin sediments were of Pliocene age and partially consolidated by compaction (Fulthorpe et al., 2010), and the Iberian margin sediments were of Quaternary age and unconsolidated (Expedition 339 Scientists, 2012; Hodell et al., 2013).

3.2. Image Analysis

3.2.1. Sample Preparation

Sample preparation is the key to obtaining good results in image analysis. Samples can be imaged in a disaggregated dispersed form (Fernlund, 2005), as a thin section (Francus, 1998), polished block (Sanei et al., 2016) or after ion milling (Milner et al., 2010). Fine-grained sediments are best imaged in polished thin sections, polished blocks or ion milled sections as this prevents overlapping of grains during imaging. The technique prevents grain breakage, which is likely to occur during sample disaggregation. It also preserves the original fabric and so allows the relationship among grains to be more accurately observed.

The two samples from Expedition 317 were allowed to dry naturally while being kept in air tight bags. The drying process was slow at room temperature. The five samples from Expedition 339 were oven dried at a controlled temperature of 60^0C until the weight of the samples remained constant regardless of further drying. The samples were vacuum impregnated with low-viscosity resin, after which polished thin sections were prepared.

3.2.2. Image acquisition

The next step after the sample has been prepared is image acquisition. The quality of the image acquired has a significant effect on image analysis end results. Accurate determination of grain size and shape estimation are dependent on the magnification of the image (Heilbronner and Barrett, 2014). Images can be acquired with a stand-alone high-resolution camera or an optical microscope with an attached camera. The choice of equipment is a

function of the grain size of the material being analysed. In geotechnical engineering, gravel-sized particles can be analysed using a high-resolution camera (Kwan et al., 1999; Lee et al., 2007). Imaging through an optical microscope is ideal for sandstone and coarse silt samples, whereas clay particle sizes are best resolved through electron microscopy. Acquired images must have a high contrast such that the boundaries between grains are clear and distinct.

Imaging of relatively large sample areas (approximately 0.65 mm by 0.42 mm) was achieved on the seven samples in this study through automated collection and stitching together of images using scanning electron microscopy (SEM) on the polished thin sections. The imaging follows a two-step procedure: (i) low resolution to get an overview of the whole polished thin section; and (ii) higher resolution of as wide an area as possible, being careful to avoid cracks or other sample disturbances (Bankole et al., 2016; Buckman, 2014). Images were acquired on a Quanta 650 FEG (field emission) SEM, operated in low vacuum (0.83 Torr), with a backscattered (BSE) detector, an operating voltage of 15 kV, spot size of 4.5 and a working distance of about 10 mm. Six randomly selected areas (or subsets) were imaged at high-resolution for each of the seven polished thin sections. The dimension of each area is approximately 650 µm by 420 µm, which is believed to be sufficiently representative of the whole sample (Fig. 3). Random selection of these areas was made in order to account for variability in the grain size from one part of the polished thin section to another. In order to more accurately analyse the very fine grain sizes, the SEM images were taken at high-resolution with about 45 nm per pixel. The smallest grain that can be technically measured at such resolution is about 135 nm; a minimum cluster of three pixels are required to confidently delineate a feature. However, particles less than 150 nm were discounted as this is close to lower end of the resolvable feature. The choice of the image resolution for the grain size analysis was informed in part by the resolution of the laser diffractometer employed (100 nm) subsequently on the subsamples of the same set.

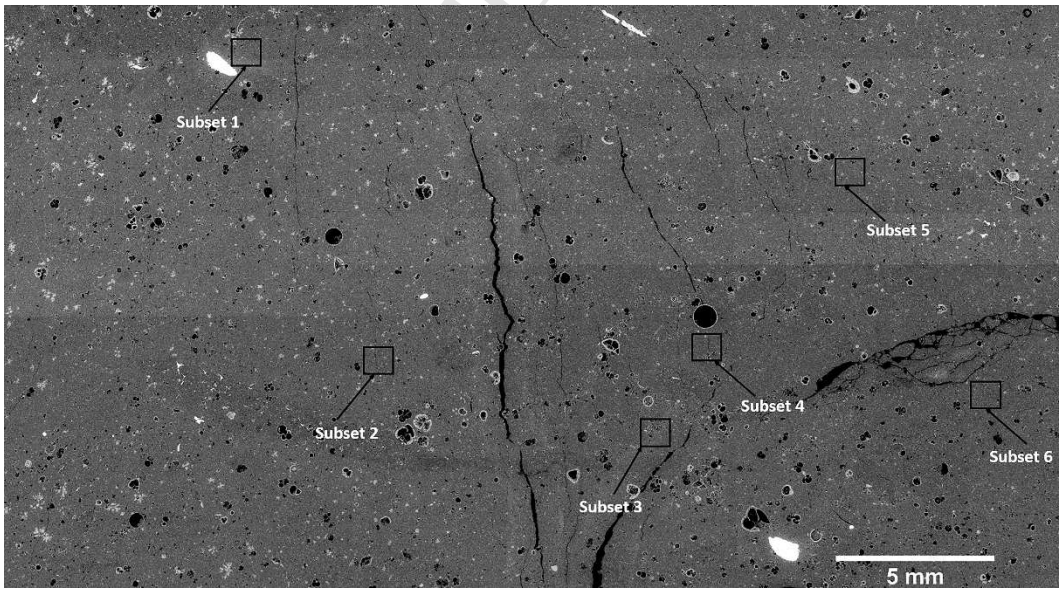

Figure 3. SEM image of sample 2 showing the six subsets of images analysed. Each subset has about 0.6 mm horizontal field of view.

3.2.3. Image processing

Image Processing of the acquired images is required to enhance certain features of the image with respect to others (Bons and Jessell, 1996). It involves enhancing the image quality to allow clear derivation of the boundary between the features through brightness and contrast adjustment, segmentation and then filtering the unwanted features (noise). The penultimate step in image processing is segmentation. In this step, features of interest are delineated from unwanted features such that the feature of interest is rendered to the foreground while unwanted features are rendered to the background. Segmentation of an image is a very important and non-trivial process (Bankole et al., 2016). For grain size analysis, the image is segmented to delineate the grains. The grains are characterised by groups of pixels and likewise the boundaries between grains. The features between the boundaries are interpreted as the grains, which are then characterised by a unique grey value. Hence, the grey value can be used to define the region occupied by the grains.

In order to enhance the boundary between the grains in this study, the images were pre-processed through the application of smooth and enhanced contrast function. After the pre-processing, each image was segmented using the default threshold, but an adjustment was made to render the grains into the foreground (black) while pores were rendered into the background (white). A median filter of the 4-pixel radius was then applied to reduce the noise and accentuate the grains (Figure 4).

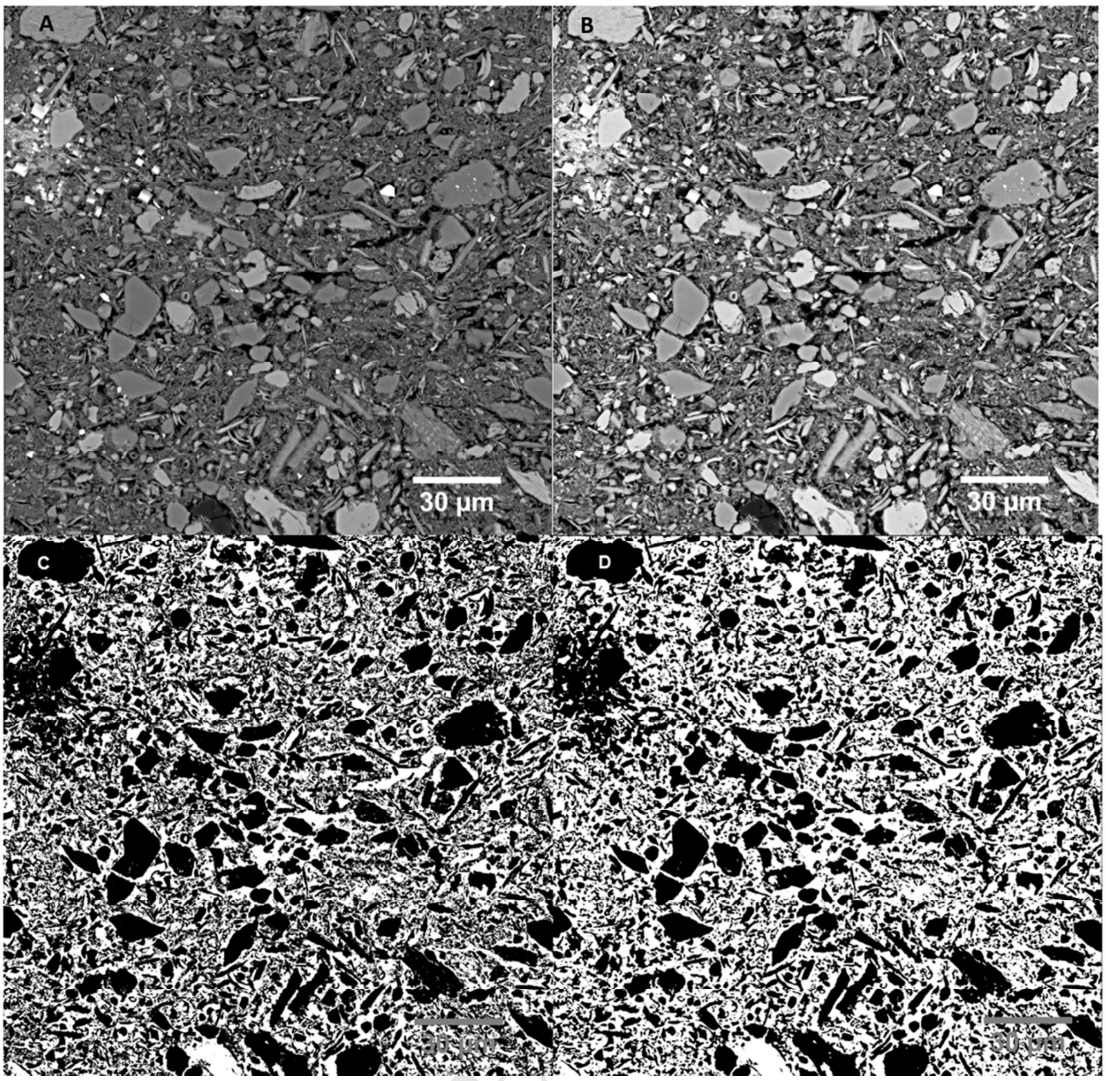

Figure 4. (A) Raw SEM image (B) SEM image after applying smoothing and contrast enhancement (C) Segmented image of grains (D) segmented image after median filtering.

3.2.4. Grain-size measurement

Grain-size measurement (or data acquisition) requires taking measurements from the processed images. Most imaging software can swiftly measure the designated areas and return grain data such as diameter, area, orientation, perimeter and others.

In this study, data on grain sizes were generated using Fiji software, which is an adaptation of *Image J*, an open software produced by the US National Institute of Health (NIH). This was first developed for analysing biological images (Schindelin et al., 2012) and it was previously known as *NIH image* software (Schneider et al., 2012). However, the usage is not limited to biological samples and the application of Fiji in the field of geoscience is gaining momentum, especially in analysing microstructure (Camp and Wawak, 2013; Hemes et al., 2015; Zhou et al., 2017).

The software is user-friendly and requires no prior knowledge of programming languages. It also provides a method for recording macros, which can be applied to several images through batch processing. Six randomly selected areas (or subsets) were imaged at high-resolution (45nm per pixel) for each of the seven polished thin sections. The dimension of each area is

approximately 650 µm by 420 µm, which is believed to be sufficiently representative of the whole sample (Figure 3). Random selection of these areas was made in order to account for variability in the grain size from one part of the polished thin section to another.

Raw images from the scanning electron microscope were processed with Fiji by first setting the scale of the image based on the horizontal field of view of the tiles in nanometers per pixel. This allowed the grain measurements to be returned in nanometers because the software does not return measurements less than one unit of the scale. Grain data were then acquired on diameter, perimeter, area, circularity, and aspect ratio. Data returned by Fiji were saved in Excel format and further data management were automated through some Excel functions and Visual Basic for Applications macros. A flowchart highlighting the steps employed in processing the image in Fiji is presented in Figure 5. Grain size was determined by measuring the Feret diameters of every grain within a one phi size class. The total number of grains was then multiplied by the phi class size and the percentage within each class was determined.

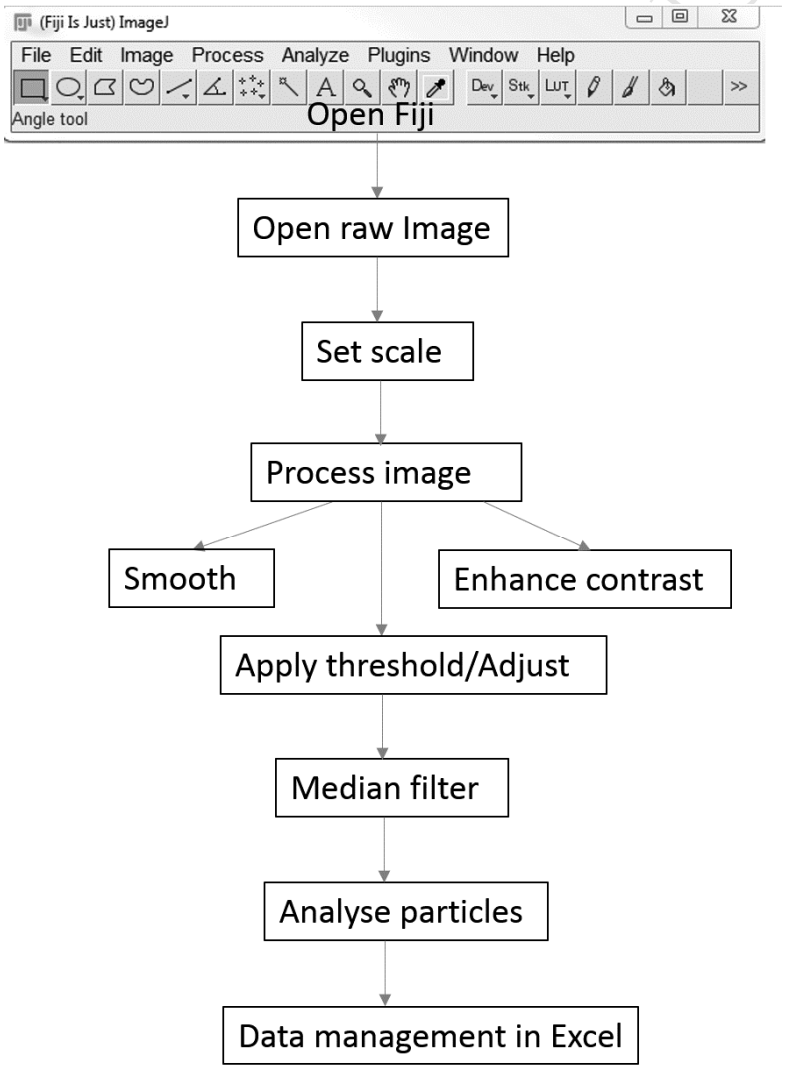

Figure 5. Flow chart highlighting the steps employed in analysing grain size with Fiji ImageJ.

3.2.5. Analysis and interpretation

The simplest method of representing grain size through image analysis is by the number of particles (frequency) recorded in each size class. However, such an approach is not comparable with most of the other methods, which record either weight or volume percentage of sediment in each size class.

Feret diameter using Fiji was measured by taking the average of multiple measurements along different grain axes. This measurement is taken as a fair representation of the particle size. Feret diameters for grain size at 1 phi intervals from 265 µm to 150 nm were calculated by summing up the diameter in each class interval. Subsequently, the percentage of Feret diameter in the class interval were determined as a measurement of percentage for each grain size class.

3.3. Laser diffraction analysis: comparative method

In order to validate the results of grain size analysis by the automated imaging technique, a subset of the same sediment samples were analysed by a standard alternative process – laser diffraction.

3.3.1. Sample preparation

Sample preparation involved suspension of an aliquot in a Calgon solution (sodium hexametaphosphate) of about 0.5 gram per litre of distilled water for 24 hours to act as a dispersant (Lewis and McConchie, 1994). Disaggregation of the samples was completed using an electrical ultrasonic probe with a long thin tip in a plastic tube. The plastic tube containing the sample was two-third filled with Calgon solution and the probe was about 1 cm above the plastic tube to prevent breakage of the tube during sonication. Complete disaggregation was achieved in about 10 to 15 mins. A subsample of the dispersed sample was introduced into the sample unit containing deionised water. The sample was then agitated in the sample unit of the granulometer to prevent flocculation during measurement.

3.3.2. Grain-size measurement

This study used a Malvern 2000 laser diffraction granulometer to measure grain sizes between 100 nm and 600 µm. The equipment has three Fourier lenses, two lenses were used for sample 1 and 2 (resolution, 100 nm – 180 µm), while a single lens with a resolution of 100 nm to 80 µm was deemed satisfactory for sample 3 to 7 based on prior knowledge of the maximum particle size expected, from earlier SEM observation.

Laser diffraction granulometry offers two calculation models which are based on two optical theories – the Fraunhofer and Mie optical theories (Beuselinck et al., 1998; Sperazza et al., 2004; Storti and Balsamo, 2010). The difference in grain sizes calculated by the two models is generally minimal, except for the finest clay size fraction (Eshel et al., 2004; Pye and Blott, 2004), for which the Fraunhofer optical model underestimates the amount of clay size particles present (Loizeau et al., 1994). This study, therefore, applied the Mie theory, which performs particularly well with homogeneous and spherical particles although not so well with more irregularly shape materials as found in many sediments (Eshel et al., 2004). The Mie theory is noted to account for more clay size particles than the commonly used Fraunhofer theory (Blott et al., 2004; Loizeau et al., 1994; Storti and Balsamo, 2010).

Statistical parameters on grain size such as mean, median, sorting, skewness among others were determined using the Gradistat software (Blott and Pye, 2001) for a single measurement based on laser diffraction.

4. Results

4.1. Subset comparison

The six subsets taken from the seven samples for image analysis show closely comparable grain-size characteristics in most cases (Table 1 and Figure 6), with little significant variation in the percentage of sand, silt and clay contents. This variation between subsets is between 1% and 6%, except for sample 3 subset 1 and 2, sample 4 subset 1 and sample 6 subset 2 in which both the silt and clay content show greater variation (up to 20%). Standard ternary grain-size plots for the all the subsets in each image shows good clustering of all subsets within the silty-mud grain-size class (Figure 7). These results show relatively homogeneous sediment samples. We can therefore take an average value from the six subsets for comparison with the laser diffraction technique.

Table 1. Summary of the results on grain size for the subset images for all the samples, from image analysis method.

Sample ID	Expedition Site/Hole	Depth	Particle size	Subset1	Subset2	Subset3	Subset4	Subset5	Subset6
Sample 1	317 1352/B	700	clay	42%	40%	43%	44%	45%	46%
			silt	52%	53%	51%	53%	53%	51%
			sand	6%	7%	6%	3%	2%	3%
Sample 2	317 1354/C	130	clay	33%	38%	35%	36%	32%	32%
			silt	65%	59%	61%	62%	65%	65%
			sand	2%	3%	4%	2%	3%	2%
Sample 3	339 1385/A	50	clay	66%	47%	53%	54%	52%	53%
			silt	34%	53%	46%	45%	47%	47%
			sand	0%	0%	1%	1%	1%	0%
Sample 4	339 1385/E	60	clay	51%	45%	43%	46%	46%	46%
			silt	48%	54%	55%	51%	52%	53%
			sand	1%	1%	1%	3%	1%	1%
Sample 5	339 1385/E	10	clay	53%	50%	52%	50%	48%	52%
			silt	45%	47%	46%	48%	48%	47%
			sand	2%	2%	2%	2%	4%	1%
Sample 6	339 1385/D	15	clay	50%	58%	50%	49%	51%	50%
			silt	48%	39%	49%	50%	48%	47%
			sand	2%	3%	1%	1%	1%	3%
Sample 7	339 1385/E	80	clay	66%	65%	66%	70%	67%	67%
			silt	33%	34%	33%	28%	32%	32%
			sand	1%	1%	1%	2%	1%	1%

322

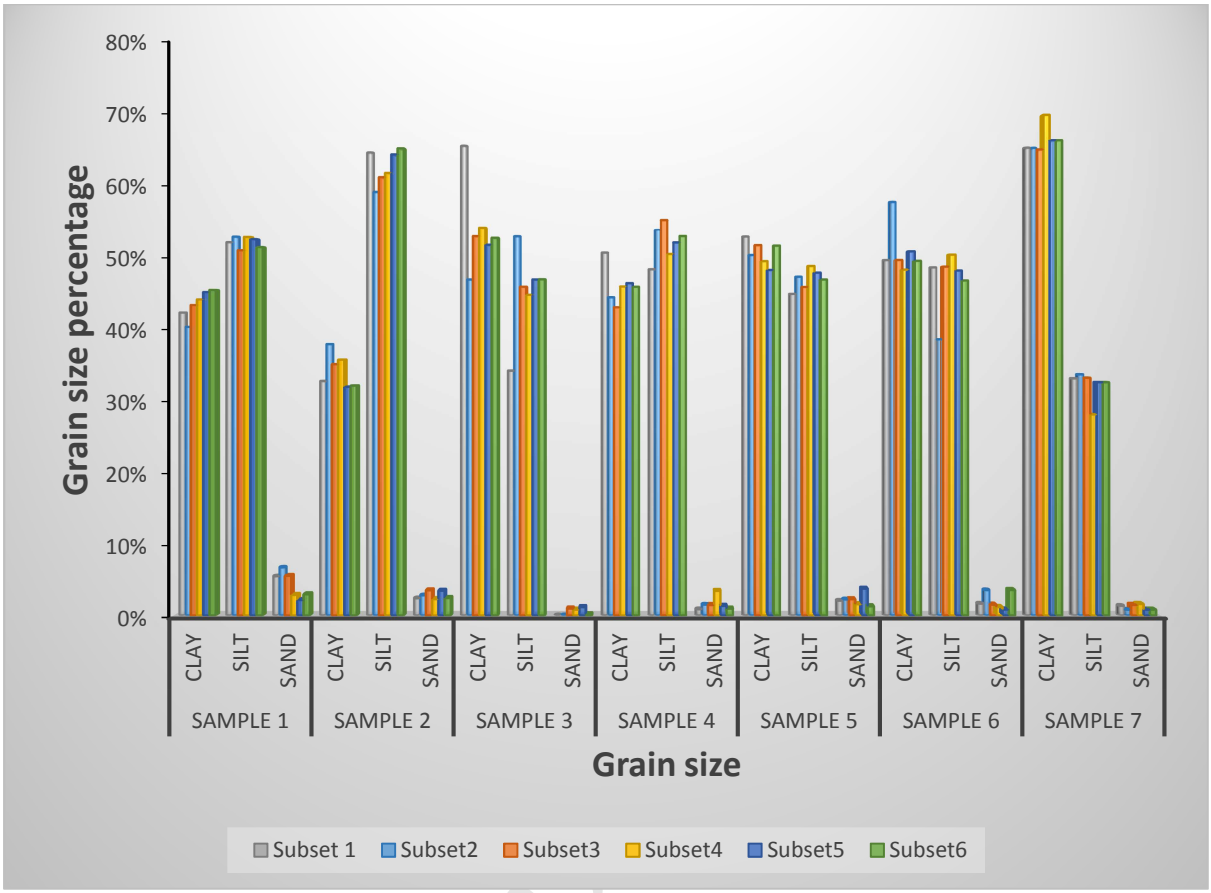

Figure 6. Grain size estimated based on Feret diameter percentage for the six subsets in each image. The variation in grain size is subtle except in sample 3 and 4 where the clay percentage in subset 1 as well as in sample 6 subset 2 is extremely higher than the other.

4.2. Comparison between techniques

The ternary grain size plots presented in Figure 7 show that the relative proportions of sand-silt-clay based on image analysis from most of the subsets and the laser technique fall within the same grain size class. This is true for samples 2, 3, and 4 where the difference in the proportion of clay is less than 12%. There is a wider variation apparent for samples 1 (with 30% variation in the clay content) and samples 5, 6 and 7 with up to 19% difference in the clay content.

The laser diffraction results are similar to image analysis results with respect to grain size classes, but there are some variation in the grain size statistical parameters between the two techniques (Figure 8). The summary results from both techniques (Table 2) indicate that all the samples are muds (within the silty-mud class) and that grain-size distributions are all unimodal. The mean grain size ranges from fine silt (7.98 phi) to very coarse silt (4.311 phi) based on both methods. There are some variation in the mean size from both techniques but generally less are than 1 phi except in sample 1 in which the difference in the mean size is up to 2 phi. In most cases where the means size varies, the mean size from the laser diffraction fall into the next coarsest grain fraction in comparison to the image analysis technique.

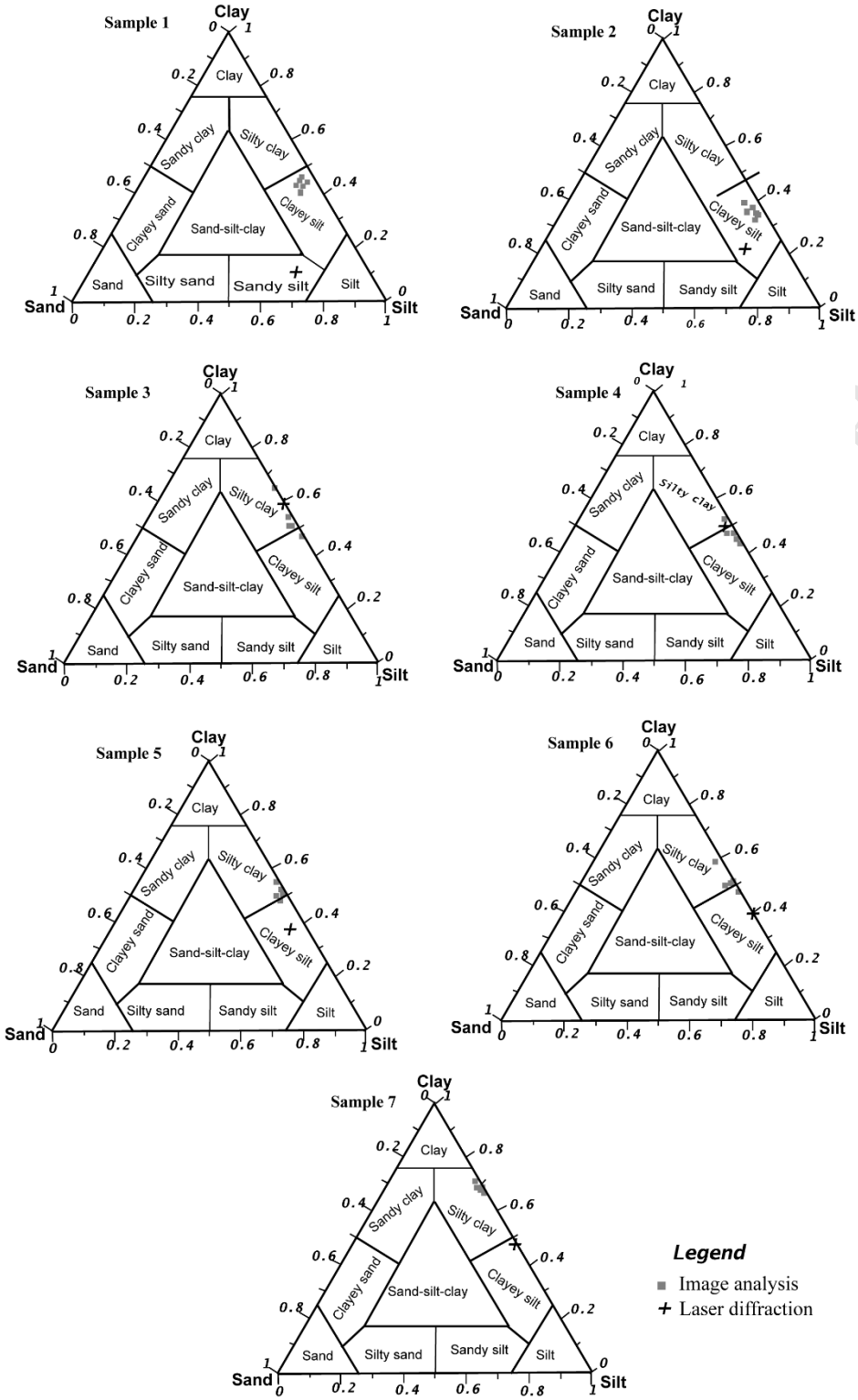

Figure 7. Ternary plot of grain size distribution (Modified from, Shepard, 1954) based on Feret diameter percentage for the various image subsets analysed and laser diffraction granulometry. The ternary plots are for samples 1 to 7 respectively. Image analysis subsets are in grey while laser diffraction results are plotted as black cross. The plots indicate grain size data from each subset within a sample. Although there is subtle variation among the subsets however, grain size composition for the varying subsets in each sample form a cluster.

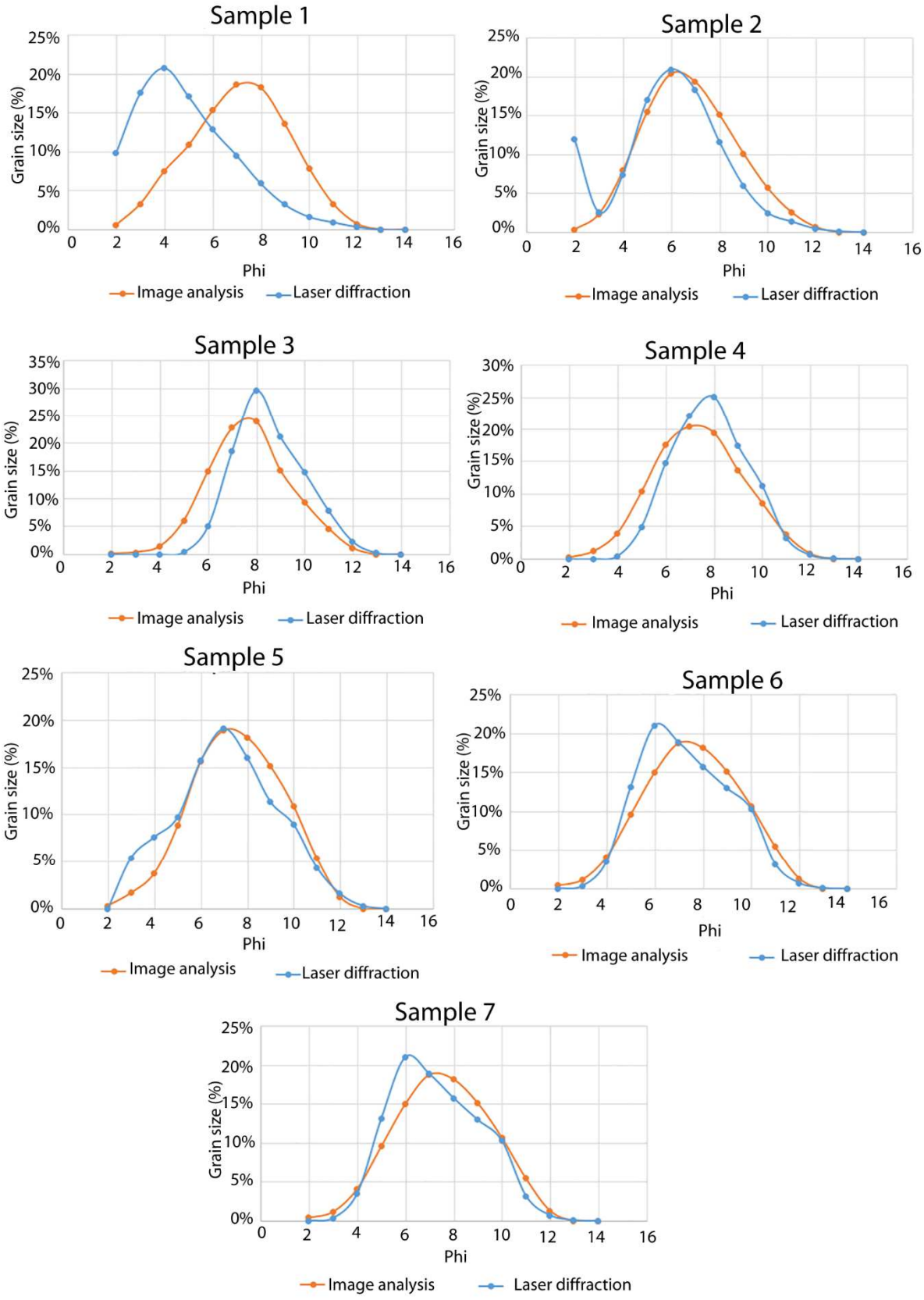

345

346 Figure 8. Grain size distribution curves to compare the results from laser diffraction
347 granulometry and image analysis technique described herein.

348 The standard deviation output from the Gradistat program, which was computed based on
349 Folk and Ward (1957), shows that the samples are very poorly sorted to poorly sorted (Table
350 2). There is no discrepancy in sorting class between the two techniques for samples 1, 3, 4
351 and 7. For samples 2, 5 and 6, the nominal difference in sorting is not more than 0.20 phi
352 units. Computed skewness for all the sample ranges from -0.048 to 0.169. Skewness based on
353 image analysis shows that the samples are symmetrical while laser diffraction shows that
354 sample 1, 2, 3 and 6 are skewed while others are symmetrical. Kurtosis determined from both
355 techniques has values between 0.852 and 1.24. The kurtosis description is the same in sample
356 1, 3, 4 and 5. However, kurtosis based on laser diffraction results shows that samples 2 is
357 leptokurtic while 6 and 7 playkurtic. Image analysis reveals that all the samples are
358 mesokurtic. The actual difference in kurtosis by comparing both techniques is less than 0.3
359 phi units in all the samples.

360 The percentage of grain size within different phi classes is plotted for both laser diffraction
361 granulometry (x-axis) and image analysis average values (y-axis) for each sample (Figure 9).
362 The plots show a strong linear positive correlation between the two techniques with an R-
363 square value of 0.76, 0.79, 0.99, 0.92, 0.91 and 0.96 for samples 2 to 7 respectively.
364 However, the R-square value for sample 1 shows no correlation between the two techniques,
365 with an R-square value of 0.083.

366

367 Table 2. Statistical parameters for results obtained from image analysis (IMA) and laser
368 diffraction (LSD) techniques using Gradistat software (Blott and Pye, 2001). The statistical
369 parameters were calculated based on Folk and Ward (1957).

Sample	Textural group	Statistical parameters					
		Mean size (phi)	Median (phi)	Distribution	Sorting	Skewness	Kurtosis
1 LSD	Mud	Very coarse silt (4.31)	Very coarse silt (4.10)	Unimodal	Very poorly sorted (2.17)	Fine skewed (0.17)	Mesokurtic (1.04)
1 IMA	Mud	Medium silt (6.56)	Medium silt (6.60)	Unimodal	Very poorly sorted (2.09)	Symmetrical (-0.0480)	Mesokurtic (0.97)
2 LSD	Mud	Coarse silt (5.38)	Coarse silt (5.50)	Unimodal	Very poorly sorted (2.30)	Coarse skewed (-0.12)	Leptokurtic (1.24)
2 IMA	Mud	Medium silt (6.24)	Medium silt (6.15)	Unimodal	Poorly sorted (1.96)	Symmetrical (0.09)	Mesokurtic (0.98)
3 LSD	Mud	Fine silt (7.99)	Fine silt (7.80)	Unimodal	Poorly sorted (1.49)	Fine skewed (0.169)	Mesokurtic (0.99)
3 IMA	Mud	Fine silt (7.18)	Fine silt (7.10)	Unimodal	Poorly sorted (1.71)	Symmetrical (0.05)	Mesokurtic (1.03)
4 LSD	Mud	Fine silt (7.29)	Fine silt (7.30)	Unimodal	Poorly sorted (1.57)	Symmetrical (0.03)	Mesokurtic (0.92)
4 IMA	Mud	Medium silt (6.84)	Medium silt (6.80)	Unimodal	Poorly sorted (1.86)	Symmetrical (0.04)	Mesokurtic (0.95)
5 LSD	Mud	Medium silt (6.58)	Medium silt (6.50)	Unimodal	Very poorly sorted (2.27)	Symmetrical (0.00)	Mesokurtic (1.01)
5 IMA	Mud	Fine silt (7.06)	Fine silt (7.00)	Unimodal	Poorly sorted (1.99)	Symmetrical (0.02)	Mesokurtic (0.94)
6 LSD	Mud	Medium silt (6.78)	Medium silt (6.60)	Unimodal	Poorly sorted (1.87)	Fine skewed (0.13)	Platykurtic (0.85)
6 IMA	Mud	Fine silt (7.04)	Fine silt (7.00)	Unimodal	Very poorly sorted (1.98)	Symmetrical (0.02)	Mesokurtic (0.93)
7 LSD	Mud	Fine silt (7.16)	Fine silt (7.10)	Unimodal	Poorly sorted (1.56)	Symmetrical (0.01)	Platykurtic (0.89)
7 IMA	Mud	Fine silt (7.05)	Fine silt (7.00)	Unimodal	Poorly sorted (1.94)	Symmetrical (0.06)	Mesokurtic (0.93)

370

371

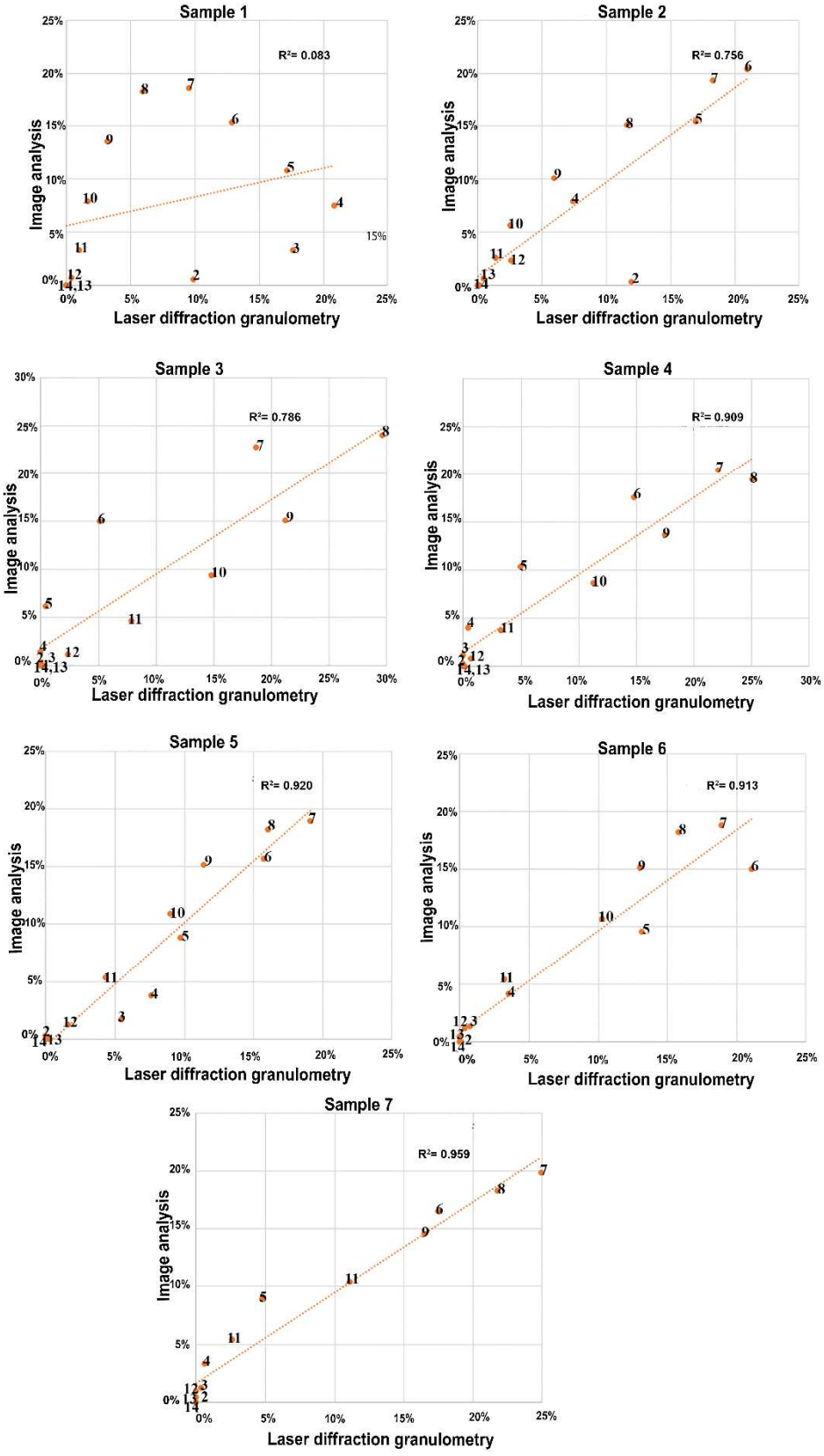

Figure 9. Plots of percentage of grain size within different phi classes for laser diffraction granulometry (x-axis) vs image analysis (y-axis) based on Feret diameter. The corresponding phi classes are written on the plotted points. Note that the average Feret diameter from six subsets of SEM images per sample was used.

5. Discussion

Grain-size measurement by image analysis is demonstrated here to be a robust and reliable technique, particularly for finer grained sediments in the clay-silt-sand size range. One possible criticism of the image analysis technique via SEM is the very small sample size that is analysed. However, the method employed in this study for image acquisition allowed for imaging of a relatively large sample area through automated collection and stitching together of images using scanning electron microscopy on the polished thin sections. The grain size was estimated from six subsets of SEM images in each sample and the number of grains analysed from each subset was between 35000 to 45000. This number of grains would have been almost impossible to manage through manual measurement.

Earlier work on grain-size analysis, typically via point-counting of thin sections, recommends measurement of about 50 to 500 grains to achieve grain size results that are statistically significant (Sanei *et al.*, 2016 and references therein). However, this approach is only viable for coarser-grained sediments (sands and gravels), and a much larger number of grains must be counted for silt and clay-sized sediment.

Image analysis is the only grain size analysis method that has the advantage over other techniques by providing a direct means of visualising grains in mudrocks with respect to the whole sediment, so that the grain shape and relationship among the grains (grain fabric) can also be determined at the same time. Grain-size analysis by other techniques mainly involve bulk analysis of disaggregated samples, and yield only the percentage of grains in each size class without having knowledge about the morphology and the number of grains considered.

The results generated in this study from image analysis were compared with samples analysed by laser diffraction granulometry. For the most part, all elements of the grain size measured, including grain-size distribution curves, ternary sand-silt-clay plots, and statistical parameters (mean size, sorting, skewness and kurtosis) are closely comparable between the two techniques. Any variation noted was only subtle, especially for 86% of the samples. There is a strong positive correlation between results from the two techniques except for one sample (sample 1), for which the correlation is very poor.

The reason for the subtle variations in grain size for most of the samples and conspicuous discrepancy in grain-size for sample 1 from laser diffraction granulometry and image analysis based on Feret diameter can be attributed to a number of reasons:

(a) Visual inspection of the SEM image for sample 1 shows that the silt particle size is dominant and embedded in the clay matrix, with very few sand grains (Figure 10). However, there are a number of conspicuous elongated particles. It is likely that the laser diffraction method overestimated the sand fraction due to the presence of the elongated particles. This is an acknowledged limitation of laser diffraction granulometry (Hayton et al., 2001; Loizeau et al., 1994; Pye and Blott, 2004).

(b) The actual samples used for image analysis and laser diffraction granulometry were necessarily different. Fine grained sediments are known to be highly heterogeneous, from the meter scale (Macquaker and Howell, 1999; Macquaker and Jones, 2002) to nanometer scale (Bernard et al., 2010; Clarkson et al., 2012; Silin and Kneafsey, 2012). There is a strong

414 possibility, therefore, that a pair of samples adjudged to be similar visually in terms of their
415 grain size and sedimentary structures, were microscopically different.

416

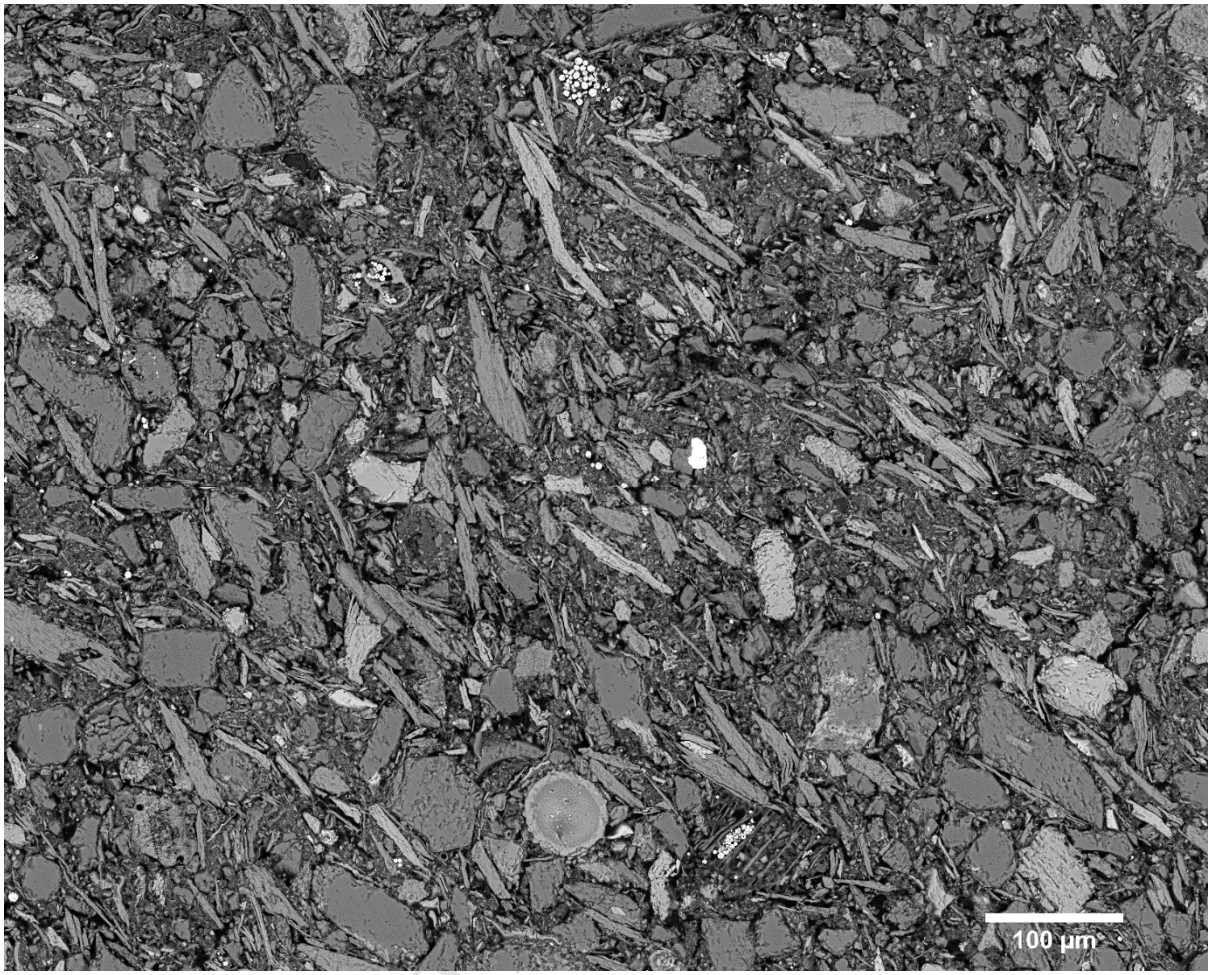

Figure 10. A subset image from sample one showing silt as the dominant grain

417

(c) It is also evident from the various subsets of images analysed herein that even in the small core plug, subtle variation exists. This is almost certainly due to sample heterogeneity at the small scale (micron to submicron scale). Laser diffraction also requires a small sample size of about 0.1g to 0.5g (Eshel et al., 2004) such that representativeness without preferential subsampling can be equally difficult using this technique.

(d) Laser diffraction granulometry requires disaggregation and dispersion of the sample, using chemical and ultrasonic treatment. Overtreatment of the sample with the ultrasonic device can result in breakage of particles, while insufficient dispersion of the sample ultrasonically can result in the reduced estimation of fine particle sizes. This might explain, in part, the common lower estimation of clay-size fraction via the laser technique.

All grain size techniques have some draw backs, and the image analysis method as described herein also has some limitations. In fact, we suggest comparison of the proposed technique with other standard techniques for analysing grain size of fine grained sediments. Firstly, the technique requires adequate segmentation and definition of grain boundaries. This is not always easy to achieve, and in some instances two grains might appear inseparable and are then measured as a single grain. In this case, there is tendency for image analysis to overestimate the coarser grain size. Secondly, image analysis in this study utilised polished thin-sections. There is possibility that individual particles might be plucked off during polishing. And, thirdly, 2-dimensional SEM images are used for the method presented here, and there is a possibility that the diameter of grains as measured is not a true representation of their 3-dimensional diameter.

In fact, grain size is a three-dimensional textural property and three-dimensional measurement is recommended for precise grain size estimation (Rubin, 2004). Quantification of grain size analysis through image analysis involves measurement in a two-dimensional image. Efforts have been made to transform grain measurement in two dimensions into three dimensions (Fernlund, 2005; Sahagian and Proussevitch, 1998). However, most transformations from two dimensions into three dimensions remains a best guess (Sanei et al., 2016), inconclusive and fraught with disagreement (Fernlund et al., 2007; Kong et al., 2005; Zhao, 1998). Most of the transformation techniques are limited to loose and coarse grained sediments (Fernlund et al., 2007) and are also susceptible to systematic error (Zhao, 1998). Adding to the degree of uncertainty associated with the transformation is the shape of the grains, which can introduce bias into the end result (Buscombe et al., 2010). Common practice involves determination of grain volume based on an assumption that the shape of the grains are spherical. However, grains in sediments are irregular and as the irregularity increases, there is a growing error between the actual diameter and estimated diameter relying on such assumptions (Syvitski et al., 1991).

6. Conclusion

This study clearly demonstrates that image analysis of polished thin sections with scanning electron microscopy is a rapid, reliable and robust method for grain-size analysis of fine-grained (mud-rich) sediments. By using automated collection and stitching together of images, it is possible to analyse relatively larger sample sizes.

460 The proposed method has the advantage of being fully automated, objective and reproducible,
461 and relatively free from human error or bias. Measuring several subsets on one sample also
462 reveals the nature and degree of heterogeneity in grain-size distribution of the sample. The
463 same samples can also be assessed for microstructure and fabric. By combining these
464 different observations, the technique becomes highly cost-effective.

465 Comparison of data from image analysis and those gained from laser diffractometry yield
466 comparable results. Minor differences are readily accounted for in terms of sediment
467 heterogeneity and in the erroneous measurement of elongate particles. Image analysis, like
468 every other technique, has its flaws and limitations, and it is always important to be cognisant
469 of these.

470 **Acknowledgements**

471 This study forms part of the Ph.D programme by SAB at Heriot-Watt University, Edinburgh,
472 and has been sponsored by the Petroleum Technology Development Fund, Nigeria. We
473 appreciate useful discussions with Professor Andy Aplin (Durham University), Yunlai Yang
474 (Saudi Aramco) and David Dewhurst (CSIRO) with respected to disaggregation of mudrocks.
475 We are also grateful to the International Ocean Discovery Program (IODP) for providing
476 access to the samples.

477

478

References

Aplin, A.C., Fleet, A.J., Macquaker, J.H.S., 1999. Muds and mudstones: Physical and fluid-flow properties. Geol. Soc. London, Spec. Publ. 158, 1–8.

Bankole, S.A., Stow, D.A. V, Lever, H., Buckman, J., 2016. Microstructure of Mudrock and the Choice of Representative Sample, in: Fifth EAGE Shale Workshop. EAGE, Catania, Italy.

Bernard, S., Horsfield, B., Schulz, H.-M., Schreiber, A., Wirth, R., Anh Vu, T.T., Perssen, F., Könitzer, S., Volk, H., Sherwood, N., Fuentes, D., 2010. Multi-scale detection of organic and inorganic signatures provides insights into gas shale properties and evolution. Chemie der Erde - Geochemistry 70, Supple, 119–133. doi:http://dx.doi.org/10.1016/j.chemer.2010.05.005

Beuselinck, L., Govers, G., Poesen, J., Degraer, G., Froyen, L., 1998. Grain-size analysis by laser diffractometry: comparison with the sieve-pipette method. CATENA 32, 193–208. doi:http://dx.doi.org/10.1016/S0341-8162(98)00051-4

Blott, S.J., Croft, D.J., Pye, K., Saye, S.E., Wilson, H.E., 2004. Particle size analysis by laser diffraction. Geol. Soc. London, Spec. Publ. 232, 63–73. doi:10.1144/gsl.sp.2004.232.01.08

Blott, S.J., Pye, K., 2001. GRADISTAT: a grain size distribution and statistics package for the analysis of unconsolidated sediments. Earth Surf. Process. Landforms 26, 1237–1248. doi:10.1002/esp.261

Bons, P., Jessell, M.W., 1996. Image analysis of microstructures in natural and experimental samples, in: Declan, G.D.P. (Ed.), Computer Methods in the Geosciences. Pergamon, pp. 135–166. doi:http://dx.doi.org/10.1016/S1874-561X(96)80014-9

Buckman, J., 2014. Use of automated image acquisition and stitching in scanning electron microscopy: Imaging of large scale areas of materials at high resolution. Microsc. Anal. 28, 13–15.

Buscombe, D., Rubin, D.M., Warrick, J.A., 2010. A universal approximation of grain size from images of noncohesive sediment. J. Geophys. Res. Earth Surf. 115, 1–17. doi:10.1029/2009JF001477

Camp, W.K., Wawak, B., 2013. Enhancing SEM grayscale images through pseudocolor conversion: Examples from eagle ford, Haynesville, and Marcellus Shales. AAPG Mem. 15–26. doi:10.1306/13391701M1021681

Clarkson, C.R., Jensen, J.L., Chipperfield, S., 2012. Unconventional gas reservoir evaluation: What do we have to consider? J. Nat. Gas Sci. Eng. 8, 9–33. doi:http://dx.doi.org/10.1016/j.jngse.2012.01.001

Curtis, M.E., Ambrose, R.J., Sondergeld, C.H., Rai, C.S., 2010. Structural characterization of gas shales on the micro- and nano-scales, in: Society of Petroleum Engineers - Canadian Unconventional Resources and International Petroleum Conference 2010. pp. 1933–1947.

Eshel, G., Levy, G.J., Mingelgrin, U., Singer, M.J., 2004. Critical Evaluation of the Use of Laser Diffraction for Particle-Size Distribution Analysis. Soil Sci. Soc. Am. J. 68, 736–743. doi:10.2136/sssaj2004.7360

Expedition 339 Scientists, 2012. Mediterranean outflow: environmental significance of the Mediterranean Outflow Water and its global implications. IODP Prelim. Report339. doi:doi:10.2204/iodp.pr.339.2012

Fernlund, J.M.R., 2005. Image analysis method for determining 3-D size distribution of coarse aggregates. Bull. Eng. Geol. Environ. 64, 159–166. doi:10.1007/s10064-004-0251-8

Fernlund, J.M.R., Zimmerman, R.W., Kragic, D., 2007. Influence of volume/mass on grain-size curves and conversion of image-analysis size to sieve size. Eng. Geol. 90, 124–137. doi:http://dx.doi.org/10.1016/j.enggeo.2006.12.007

Folk, R.L., Ward, W.C., 1957. Brazos River bar: A study in the significance of grain size parameters. J. Sediment. Petrol. 27, 3–26.

Francus, P., 1998. An image-analysis technique to measure grain-size variation in thin sections of soft clastic sediments. Sediment. Geol. 121, 289–298. doi:http://dx.doi.org/10.1016/S0037-0738(98)00078-5

Fulthorpe, C.S., Hoyanagi, K., Blum, P., Guèrin, G., Slagle, A.L., Blair, S.A., Browne, G.H., Carter, R.M., Ciobanu, M.C., Claypool, G.E., Crundwell, M.P., Dinarès-Turell, J., Ding, X., George, S.C., Hepp, D.A., Jaeger, J., Kawagata, S., Kemp, D.B., Kim, Y.G., Kominz, M.A., Lever, H., Lipp, J.S., Marsaglia, K.M., McHugh, C.M., Murakoshi, N., Ohi, T., Pea, L., Richaud, M., Suto, I., Tanabe, S., Tinto, K.J., Uramoto, G., Yoshimura, T., 2010. Integrated ocean drilling program expedition 317 preliminary report canterbury basin sea level global and local controls on continental margin stratigraphy. Integr. Ocean Drill. Progr. Prelim. Reports 1–133.

Hayton, S., Nelson, C.S., Ricketts, B.D., Cooke, S., Wedd, M.W., 2001. Effect of mica on particle-size analyses using the laser diffraction technique. J. Sediment. Res. 71, 507–509.

Heilbronner, R., Barrett, S., 2014. Image analysis in earth sciences: Microstructures and textures of earth materials, Image Analysis in Earth Sciences: Microstructures and Textures of Earth Materials. Springer Berlin Heidelberg. doi:10.1007/978-3-642-10343-8

Hemes, S., Desbois, G., Urai, J.L., Schröppel, B., Schwarz, J.-O., 2015. Multi-scale characterization of porosity in Boom Clay (HADES-level, Mol, Belgium) using a combination of X-ray μ-CT, 2D BIB-SEM and FIB-SEM tomography. Microporous Mesoporous Mater. 208, 1–20. doi:http://dx.doi.org/10.1016/j.micromeso.2015.01.022

Hodell, D.A., Lourens, L., Stow, D.A. V, Hernández-Molina, J., Alvarez Zarikian, C.A., Abrantes, F., Acton, G.D., Bahr, A., Balestra, B., Llave Barranco, E., Carrara, G., Crowhurst, S., Ducassou, E., Flood, R.D., Flores, J.A., Furota, S., Grimalt, J., Grunert, P., Jimenez-Espejo, F.J., Kyoung Kim, J., Konijnendijk, T., Krissek, L.A., Kuroda, J., Li, B., Lofi, J., Margari, V., Martrat, B., Miller, M.D., Nanayama, F., Nishida, N., Richter, C., Rodrigues, T., Rodríguez-Tovar, F.J., Freixo Roque, A.C., Sanchez Goni, M.F., Sierro Sánchez, F.J., Singh, A.D., Skinner, L., Sloss, C.R., Takashimizu, Y., Tjallingii, R., Tzanova, A., Tzedakis, C., Voelker, A., Xuan, C., Williams, T., 2013. The "Shackleton Site" (IODP Site U1385) on the Iberian Margin. Sci. Drill. 13–19. doi:10.5194/sd-16-13-2013

Ji, W., Song, Y., Rui, Z., Meng, M., Huang, H., 2017. Pore characterization of isolated

organic matter from high matured gas shale reservoir. Int. J. Coal Geol. 174, 31–40. doi:10.1016/j.coal.2017.03.005

Jiang, Z., Liu, L., 2011. A pretreatment method for grain size analysis of red mudstones. Sediment. Geol. 241, 13–21. doi:http://dx.doi.org/10.1016/j.sedgeo.2011.09.008

Kong, M., Bhattacharya, R.N., James, C., Basu, A., 2005. A statistical approach to estimate the 3D size distribution of spheres from 2D size distributions. Geol. Soc. Am. Bull. 117, 244–249. doi:10.1130/b25000.1

Kwan, A.K.H., Mora, C.F., Chan, H.C., 1999. Particle shape analysis of coarse aggregate using digital image processing. Cem. Concr. Res. 29, 1403–1410. doi:http://dx.doi.org/10.1016/S0008-8846(99)00105-2

Lee, J.R.J., Smith, M.L., Smith, L.N., 2007. A new approach to the three-dimensional quantification of angularity using image analysis of the size and form of coarse aggregates. Eng. Geol. 91, 254–264. doi:http://dx.doi.org/10.1016/j.enggeo.2007.02.003

Lewis, D.W., McConchie, D.M., 1994. Analytical Sedimentology. Chapman & Hall, Great Britain.

Loizeau, J.L., Arbouille, D., Santiago, S., Vernet, J.P., 1994. Evaluation of a wide range laser diffraction grain size analyser for use with sediments. Sedimentology 41, 353–361. doi:10.1111/j.1365-3091.1994.tb01410.x

Macquaker, J.H.S., Howell, J.K., 1999. Small-scale (< 5.0 m) vertical heterogeneity in mudstones: implications for high-resolution stratigraphy in siliciclastic mudstone successions. J. Geol. Soc. London. 156, 105–112.

Macquaker, J.H.S., Jones, C.R., 2002. A sequence-stratigraphic study of mudstone heterogeneity: a combined petrographic/wireline log investigation of Upper Jurassic Mudstones from the North Sea (UK). Geol. Appl. Well Logs. AAPG Methods Explor. Ser. 13, 123–141.

Malverns Instruments Limited, 2012. A basic guide to particle characterization.

Milner, M., McLin, R., Petriello, J., 2010. Imaging Texture and Porosity in Mudstones and Shales: Comparison of Secondary and Ion-Milled Backscatter SEM Methods, in: Canadian Unconventional Resources and International Petroleum Conference. doi:10.2118/138975-MS

Pye, K., Blott, S.J., 2004. Particle size analysis of sediments, soils and related particulate materials for forensic purposes using laser granulometry. Forensic Sci. Int. 144, 19–27. doi:10.1016/j.forsciint.2004.02.028

Røgen, B., Gommesen, L., Fabricius, I.L., 2001. Grain size distributions of chalk from image analysis of electron micrographs. Comput. Geosci. 27, 1071–1080. doi:http://dx.doi.org/10.1016/S0098-3004(00)00159-X

Rubin, D.M., 2004. A simple autocorrelation algorithm for determining grain size from digital images of sediment. J. Sediment. Res. 74, 160–165. doi:10.1306/052203740160

Sahagian, D.L., Proussevitch, A.A., 1998. 3D particle size distributions from 2D observations: Stereology for natural applications. J. Volcanol. Geotherm. Res. 84, 173–196. doi:10.1016/S0377-0273(98)00043-2

606 Sanei, H., Ardakani, O.H., Ghanizadeh, A., Clarkson, C.R., Wood, J.M., 2016. Simple
607 petrographic grain size analysis of siltstone reservoir rocks: An example from the
608 Montney tight gas reservoir (Western Canada). Fuel 166, 253–257.
609 doi:http://dx.doi.org/10.1016/j.fuel.2015.10.103

610 Saner, S., Cagatay, M.N., Al Sanounah, A.M., 1996. Relationships between shale content and
611 grain-size parameters in the Safaniya Sandstone reservoir, NE Saudi Arabia. J. Pet.
612 Geol. 19, 305–320. doi:10.1111/j.1747-5457.1996.tb00436.x

613 Saraji, S., Piri, M., 2015. The representative sample size in shale oil rocks and nano-scale
614 characterization of transport properties. Int. J. Coal Geol. 146, 42–54.
615 doi:http://dx.doi.org/10.1016/j.coal.2015.04.005

616 Schindelin, J., Arganda-Carreras, I., Frise, E., Kaynig, V., Longair, M., Pietzsch, T.,
617 Preibisch, S., Rueden, C., Saalfeld, S., Schmid, B., Tinevez, J.Y., White, D.J.,
618 Hartenstein, V., Eliceiri, K., Tomancak, P., Cardona, A., 2012. Fiji: an open-source
619 platform for biological-image analysis. Nat. Methods 9, 676–682.
620 doi:10.1038/nmeth.2019

621 Schneider, C.A., Rasband, W.S., Eliceiri, K.W., 2012. NIH Image to ImageJ: 25 years of
622 image analysis. Nat. Methods 9, 671–675.

623 Shepard, F.P., 1954. Nomenclature Based on Sand-silt-clay Ratios. SEPM J. Sediment.
624 Petrol. 24, 151–158. doi:10.1306/D4269774-2B26-11D7-8648000102C1865D

625 Silin, D., Kneafsey, T., 2012. Shale Gas: Nanometer-Scale Observations and Well Modelling.
626 J. Can. Pet. Technol. 51, 464–475.

627 Sperazza, M., Moore, J.N., Hendrix, M.S., 2004. High-resolution particle size analysis of
628 naturally occurring very fine-grained sediment through laser diffractometry. J. Sediment.
629 Res. 74, 736–743. doi:10.1306/031104740736

630 Storti, F., Balsamo, F., 2010. Particle size distributions by laser diffraction: Sensitivity of
631 granular matter strength to analytical operating procedures. Solid Earth 1, 25–48.

632 Syvitski, J.P.M., Leblanc, K.W.G., Asprey, K.W., 1991. Interlaboratory, interinstrument
633 calibration experiment, in: Syvitski, J.P.M. (Ed.), Principles, Methods and Application
634 of Particle Size Analysis. Cambridge University Press, Cambridge, UK, pp. 174–193.

635 Wentworth, C.K., 1922. A scale of grade and class terms for clastic sediments. J. Geol. 30,
636 377–392.

637 Yang, Y., Aplin, A.C., 2007. Permeability and petrophysical properties of 30 natural
638 mudstones. J. Geophys. Res. Solid Earth 112. doi:10.1029/2005JB004243

639 Zhao, X.B., 1998. Measurement and calculation of three-dimensional grain sizes and size
640 distribution functions. Microsc. Microanal. 4, 420–427.

641 Zhou, S., Liu, D., Cai, Y., Yao, Y., Li, Z., 2017. 3D characterization and quantitative
642 evaluation of pore-fracture networks of two Chinese coals using FIB-SEM tomography.
643 Int. J. Coal Geol. 174, 41–54. doi:10.1016/j.coal.2017.03.008

644

- Grain size has significant effect on petrophysical properties of the rock.
- Characterising mudrocks is challenging as conventional methods are unsuitable.
- The technique presented gives comparable grain size results with laser diffraction.
- Grain size from SEM image as described here is rapid and cost effective.